



Available online at www.sciencedirect.com

ScienceDirect

Geochimica et Cosmochimica Acta 181 (2016) 1-17

Geochimica et Cosmochimica Acta

www.elsevier.com/locate/gca

Colloidal size spectra, composition and estuarine mixing behavior of DOM in river and estuarine waters of the northern Gulf of Mexico

Zhengzhen Zhou a,b, Björn Stolpe a,c, Laodong Guo a,b,*, Alan M. Shiller a

a Department of Marine Science, University of Southern Mississippi, Stennis Space Center, MS 39529, USA
 b School of Freshwater Sciences, University of Wisconsin-Milwaukee, 600 East Greenfield Avenue, Milwaukee, WI 53204, USA
 c Akzo Nobel Pulp & Performance Chemicals, 445 80 Bohus, Sweden

Received 23 November 2014; accepted in revised form 28 February 2016; available online 3 March 2016

Abstract

Flow field-flow fractionation (FIFFF) coupled on-line with UV absorbance and fluorescence detectors was used to examine the colloidal composition and size distribution of optically active dissolved organic matter (DOM) in the lower Mississippi River (MR), the East Pearl River (EPR), the St. Louis Bay (SLB) estuary, and coastal waters of the northern Gulf of Mexico. In addition to field studies, laboratory mixing experiments using river and seawater end-members were carried out to study the processes controlling the estuarine mixing behavior and size partitioning of colloids with different sizes and composition. The colloidal size spectra of chromophoric DOM and humic-like DOM showed one dominant peak in the 0.5-4 nm size range, representing >75% of the total FIFFF-recoverable colloids. In contrast, protein-like DOM showed a bi-modal distribution with peaks at 0.5–4 nm and 4–8 nm, as well as a major portion (from \sim 41% in the EPR to \sim 72% in the Mississippi Bight) partitioned to the >20 nm size fraction. Bulk DOM was lower in abundance and molecular-weight in the MR compared with the EPR, while the proportion of colloidal protein-like DOM in the >20 nm size range was slightly larger in the MR compared with the EPR. These features are consistent with differences in land use, hydrological conditions, and water residence time between the two river basins, with more autochthonous DOM in MR waters. In the SLB estuary, different DOM components demonstrated different mixing behaviors. The abundance of colloidal chromophoric DOM decreased with increasing salinity and showed evident removal during estuarine mixing even though the bulk DOM appeared to be conservative. In contrast, colloidal humic-like DOM behaved conservatively inside SLB and during laboratory mixing experiments. The ratio of colloidal protein-like to humic-like DOM generally increased with increasing salinity, consistent with increasing autochthonous protein-like DOM and removal of terrestrially-derived humic-like DOM in estuarine and coastal waters. Similar mixing behavior for the bulk DOM and colloids was observed in short-term laboratory mixing experiments, suggesting that physicochemical processes are the major controlling factor for colloidal removal in the estuary. For the first time, this study showed direct evidence of contrasting estuarine mixing behavior for different size fractions of optically active colloidal DOM.

© 2016 Elsevier Ltd. All rights reserved.

E-mail address: guol@uwm.edu (L. Guo).

1. INTRODUCTION

Dissolved organic matter (DOM) is a major component of the global carbon cycle and plays an important role in regulating the biogeochemical cycling of nutrients and trace

^{*} Corresponding author at: School of Freshwater Sciences, University of Wisconsin-Milwaukee, 600 East Greenfield Avenue, Milwaukee, WI 53204, USA. Tel.: +1 414 382 1742.

elements in aquatic systems (Hedges, 2002; Aiken et al., 2011; Bauer et al., 2013). The bulk DOM has been shown to be heterogeneous in size, composition, and chemical reactivity (Guo et al., 1996; Hansell, 2013; Benner and Amon, 2015). Among various sizes of DOM components, bulk DOM is composed of mostly colloidal organic matter or high-molecular-weight (HMW) DOM, especially in freshwater and estuarine environments (Guo and Santschi, 2007; Cai and Guo, 2009).

Colloidal organic matter, operationally defined as the >1 kDa fraction of DOM (Guo and Santschi, 2007), has been found to contain a variety of compounds and act as a dynamic intermediary between dissolved and particulate phases and regulates the transfer of some reactive metal ions to particles (Honeyman and Santschi, 1989; Guo and Santschi, 1997a). It also plays a critical role in regulating the concentration and speciation, and hence the fate, transport and bioavailability of trace metals and pollutants in aquatic systems (Benedetti et al., 2003; Lead and Wilkinson, 2006; Aiken et al., 2011; Philippe and Schaumann, 2014). The size of colloidal DOM determines its utilization efficiency by microbes (Amon and Benner, 1996). Nevertheless, knowledge of the composition and size partitioning of colloidal DOM remains scarce, even though it should provide insights into the biogeochemical cycling pathways of DOM and trace elements in aquatic environments (Stolpe et al., 2010; Stolpe et al., 2013; Philippe and Schaumann, 2014).

Flow field-flow fractionation (FlFFF) chromatography-like technique in which the retention force is provided by a cross-flow perpendicular to the channelflow, and colloids are separated based on their diffusion coefficients (Giddings, 1993). A variety of detection systems, such as UV-absorbance and fluorescence, have been coupled online with FIFFF to examine the continuous colloidal size spectra of natural organic matter (Zanardi-Lamardo et al., 2002; Stolpe et al., 2010; Guéguen and Cuss, 2011). Although applications of FIFFF to the investigation of the size distribution of natural DOM and nanoparticles in aquatic systems have been increasing (e.g., Baalousha et al., 2011; Zhou and Guo, 2015), studies focusing on dynamic variability of colloidal organic matter during estuarine mixing are still few.

Estuaries are a dynamic aquatic environment where river water meets seawater and where changes in salinity, pH, turbidity, and DOM sources are the most dramatic (Bianchi, 2007). Many previous studies have investigated the mixing behavior of bulk dissolved organic carbon (DOC) in different estuaries, including the St. Louis Bay estuary (Mississippi), showing both conservative and nonconservative mixing behavior (e.g., Sholkovitz, 1976; Mantoura and Woodward, 1983; Guo et al., 1999; Wang et al., 2010). Wang et al. (2010) also showed that carbohydrate DOM components could be preferentially removed during estuarine mixing although the bulk DOC was somewhat conservative. It is likely that different sized colloidal DOM components may also behave differently during estuarine mixing due to their differences in composition and reactivity. Unfortunately, the estuarine mixing behavior of colloids with different sizes and composition remains poorly understood. Approaches combining both field studies and laboratory mixing experiments and using techniques capable of continuum separation and characterization of colloids are needed.

Our FIFFF system was coupled with both UV absorbance and fluorescence detectors targeting the chromophoric, humic-like and protein-like DOM components. Size spectra of colloidal DOM and their variations were examined and compared between two rivers, the lower Mississippi River (MR), a large river with a massive drainage basin and extensive anthropogenic influence (Beckett and Pennington, 1986; Wiener et al., 1996), and the Lower Pearl River (PR), a small black-water river that is less anthropogenically impacted (Duan et al., 2007a,b). In addition, DOM composition and size spectra were determined in samples from the St. Louis Bay (SLB) estuary; the Mississippi Sound (MS), a nearshore water body that receives influence from the PR; and the Mississippi Bight (MB), a coastal water influenced by the MR, in the northern Gulf of Mexico. Furthermore, laboratory mixing experiments mimicking the estuarine mixing process were carried out and compared with the field results, in order to examine the estuarine mixing behavior of colloids with different sizes and composition. Our study provides insights into how the abundance and size distribution of different types of colloids are influenced by hydrological conditions and land use in river basins, and what major biogeochemical processes and mechanisms control size distribution and mixing behavior of colloidal DOM in estuarine environments.

2. MATERIALS AND METHODS

2.1. Study sites

The Mississippi River (MR), with an average flow rate of 17,000 m³/s and a drainage basin covering about 40% of the contiguous United States (\sim 3,220,000 km²), is the fourth longest (3770 km) river in the world. Cropland covers about 58% of its drainage basin (Goolsby et al., 2000; Goolsby and Battaglin, 2001), and the river is largely constrained by dam systems and levees (Keown et al., 1986; Meade et al., 1990). Decreased suspended sediment and increased nutrients, organic contaminants and trace elements in the recent past have caused eutrophication, hypoxia and other environmental issues in the northern Gulf of Mexico (Boesch et al., 2009; Duan et al., 2013). The Pearl River (PR), in contrast, is a small 3rd order black-water river that is less perturbed by human activities compared with the MR. The Pearl River is 790 km long with a total drainage area of about 22,690 km² covering east-central Mississippi and southeastern Louisiana. The most important land type in the PR basin is natural forest $(\sim 43\%)$, followed by agricultural regions (27%) and marsh and/or swamp areas (\sim 10%). Our sampling station was on the East Pearl River (EPR) near the Stennis Space Center, the same sampling location as in many previous studies (e.g., Duan and Bianchi, 2006; Duan et al., 2007b; Cai and Guo, 2009; Shiller et al., 2012; Wang et al., 2013), which have provided rich background information on DOM concentrations and composition and their spatial

and temporal variations. Shiller et al. (2012) pointed out that, during low discharge, Hobolochitto Creek may become the primary water source at the EPR depending on the specific sampling time. However, previous studies have found that both DOC abundance and DOM composition did not show significant difference between sampling stations on the EPR and a PR mainstem station at Bogalusa, MS although spatial variation along the upper river was observed (e.g., Duan and Bianchi, 2006; Duan et al., 2007b).

St. Louis Bay (SLB) is a shallow semi-closed estuary located on the Mississippi Gulf Coast, receiving freshwater inputs from the Jourdan River (JR) and the Wolf River, which are black-water, forested rivers with limited human influence (Fig. 1). The abundance, distribution, and mixing behaviors of nutrients and organic carbon in the SLB estuary have recently been reported (Wang et al., 2010; Cai et al., 2012; Lin et al., 2012). The SLB connects to the Gulf of Mexico through the Mississippi Sound (MS), where estuarine waters from SLB further mix with seawater (Fig. 1). Additionally, the PR empties into the MS (Chigbu et al., 2005) and the MR provides a portion of the water sources into the Mississippi Bight (MB) in the northern Gulf of Mexico (Blumberg et al., 2001; Morey et al., 2003; Brunner et al., 2006).

Samples from the two contrasting rivers were used to examine linkages among colloidal size/composition, DOM sources and river settings, while the estuarine samples should reveal the dynamic change in colloidal size and composition across the river-sea interface.

2.2. Sample collection

Monthly water samples were collected between January 2009 and February 2010 from the lower MR near the USGS hydrological station at Baton Rouge, Louisiana (30°26'17.01" N, 91°11'33.14" W) and from the EPR at Stennis Space Center, Mississippi (30°20′55.52″ N, 89° 38'28.74" W, Table 1, Fig. 1). Time series samples from these two rivers should provide coupled information on DOM characteristics and hydrological conditions. Water samples were also collected along a salinity gradient from the JR (30°23′12" N, 89°27′46" W), through the SLB estuary, to the MS and the MB during October 2009 (Table 2, Fig. 1), to provide the first data set of DOM size distribution in the SLB estuary. For laboratory mixing experiments, end-member river water was collected from the JR, but on a different day from the field salinity gradient sampling, and end-member seawater from the MB in the northern Gulf of Mexico (Table 2, Fig. 1).

Discharge data at the hydrological stations at Baton Rouge for the lower MR and at Bogalusa for the PR were acquired from the USGS national water information system website (http://waterdata.usgs.gov/nwis/rt). There is no routinely measured discharge for the EPR. Thus, reported PR discharge here only provides a general indication of the variation pattern of the discharge due to the complex hydrology of the EPR system (Shiller et al., 2012).

Large volumes of surface water samples (\sim 40 L) were filtered *in situ* through a 0.45 μ m Memtrex polycarbonate pleated cartridge (GE Water and Process Technologies)

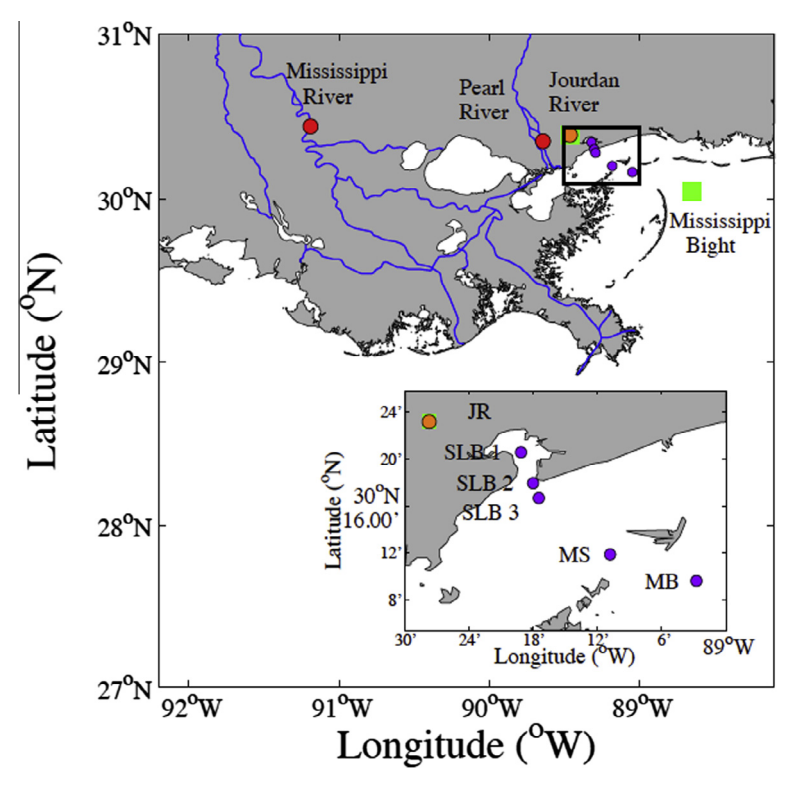


Fig. 1. Sampling locations in the lower Mississippi River (MR) at Baton Rouge, Louisiana; the East Pearl River (EPR) near Stennis Space Center, Mississippi; the Jourdan River (JR); and St. Louis Bay (SLB), the Mississippi Sound (MS), and Mississippi Bight (MB) in the northern Gulf of Mexico.

Table 1 Hydrographic parameters and concentrations of dissolved organic carbon (DOC) and colloidal organic carbon (COC) in samples from the lower Mississippi River (MR) and the East Pearl River (PR).

Sample ID	Sampling date	Discharge (m ³ /s)	Specific conductivity (µS/cm)	Temp (°C)	DOC (µM)	COC (µM)	COC/DOC (%)
MR	23-Jan-09	16,622	382	6.3	256 ± 1	151	59
MR	20-Feb-09	14,926	343	8.8	236 ± 2	_	_
MR	27-Mar-09	18,774	314	13	324 ± 2	183	57
MR	24-Apr-09	21,345	350	15.9	296 ± 2	_	_
MR	29-May-09	34,688	308	36.7	339 ± 2	204	60
MR	29-Jun-09	19,658	326	29.8	317 ± 2	_	_
MR	30-Jul-09	10,395	388	27.8	270 ± 2	_	_
MR	26-Aug-09	9047	391	28.8	264 ± 2	_	_
MR	29-Sep-09	11,771	330	25.6	299 ± 4	182	61
MR	29-Oct-09	20,445	276	16.1	343 ± 2	_	_
MR	30-Nov-09	20,048	324	13	337 ± 2	_	_
MR	31-Dec-09	22,283	267	7	265 ± 1	_	_
MR	28-Jan-10	17,695	355	7.3	275 ± 1	167	61
MR	25-Feb-10	25,482	290	5.7	237 ± 1	_	_
PR	15-Jan-09	1189	48	10.3	728 ± 2	_	_
PR	13-Feb-09	127	_	16	376 ± 1	_	_
PR	14-Mar-09	96	78	21.7	326 ± 1	_	_
PR	2-Apr-09	2011	37	18.8	1121 ± 5	_	_
PR	7-Apr-09	1470	39	17.5	834 ± 3	604	72
PR	2-May-09	116	75	27.4	438 ± 2	_	_
PR	22-May-09	289	60	24.9	666 ± 3	_	_
PR	23-Jun-09	66	238	32.8	398 ± 3	_	_
PR	15-Jul-09	56	2500	31	353 ± 2	_	_
PR	17-Aug-09	65	4470	30.4	617 ± 3	_	_
PR	23-Sep-09	94	266	28.3	899 ± 2	_	_
PR	26-Oct-09	881	80	17.7	889 ± 2	_	_
PR	25-Nov-09	114	83	18.2	569 ± 1	_	_
PR	28-Dec-09	943	39	9.8	790 ± 2	_	_
PR	31-Jan-10	983	48	10.5	736 ± 2	_	_
PR	25-Feb-10	428	38	11.3	579 ± 2	_	_

Table 2 Salinity and concentrations of DOC and COC in end-member water samples used for laboratory mixing experiments and in samples from the St. Louis Bay (SLB), Jourdan River (JR), and Mississippi Sound (MS), and Mississippi Bight (MB).

Sample ID	Sampling date	Latitude (°N)	Longitude (°W)	Salinity	$DOC (\mu M)$	$COC (\mu M)$	COC/DOC (%)
JR	Oct 06 2009	30°23′12″	89°27′46″	0.1	1618 ± 4	1107	68
SLB 1	Oct 15 2009	30°20′35″	89°19′10″	4.9	1176 ± 5	665	57
SLB 2	Oct 15 2009	30°17′58″	89°18′2″	9.8	752 ± 3	390	52
SLB 3	Oct 15 2009	30°16′42″	89°17′30″	14.5	421 ± 1	189	45
MS	Oct 15 2009	30°11′53″	89°10′50″	18	390 ± 3	167	43
MB	Oct 15 2009	30°9′37″	89°2′45″	26	234 ± 2	99	45
JR	Jan 13 2010	30°23′12″	89°27′46″	0.1	387 ± 3	_	_
MB	Jan 13 2010	30°2′35″	88°39'02"	30	154 ± 1	_	_

for ultrafiltration (see below). Aliquots of filtered waters were collected in pre-combusted glass vials for the measurements of DOC and in HDPE plastic bottles for FIFFF analysis. Samples were kept in an iced cooler and transported back to the lab within 2–3 h of collection and stored in the dark at 2 °C until further analysis. Water temperature and salinity were measured with a YSI water quality sonde at the time of sample collection.

2.3. Ultrafiltration

Ultrafiltration was used to quantify the concentration of bulk colloidal organic carbon (COC). An ultrafiltration membrane having a nominal MW cutoff of 1 kilo-Dalton (kDa), which corresponds to \sim 1.3 nm in size (Guo and Santschi, 2007), was used. Time-series permeate (<1 kDa) samples were collected at different concentration factors (CF) and were determined for DOC concentration to quantify the COC abundance (or percentage) in the bulk DOC (Guo and Santschi, 1996; Guo and Santschi, 2007), by fitting the time-series permeate DOC concentration (C_p) against CF:

$$\ln C_p = \ln(P_c \times C_f^0) + (1 - P_c) \times \ln(CF)$$

where P_c is the permeation coefficient of low-molecularweight (LMW) or permeable DOC, defined as the ratio of C_p to C_f (feed concentration of permeable DOC), and C_f^0 is its initial feed concentration. DOC recovery from permeate and retentate was, on average, $98 \pm 2\%$ for all samples.

2.4. Measurements of DOC and UV-vis absorbance

Concentrations of DOC were measured with a Shimadzu TOC-V total organic carbon analyzer using the high temperature combustion method (Guo et al., 1995). Calibration curves were generated before sample analysis. Samples were acidified with concentrated HCl to pH \leq 2 before analysis. Each sample was determined with three to five replicates, each using 150 µL, with a coefficient of variance < 2%. Ultrapure water, working standards and certified DOC standards (from University of Miami) were measured every eight samples to check the performance of the instrument and to ensure data quality (Zhou et al., 2013). The UV-vis absorption spectra of samples were measured on a Cary 300 Bio UV-vis spectrophotometer in 1-cm quartz cuvettes over 200-1100 nm with 1 nm increments (Zhou et al., 2013). Samples with absorbance higher than 0.02 at 260 nm were diluted with ultrapure water (18.2 M Ω) to reach absorbance <0.02 in order to minimize the inner-filter effect (Coble et al., 1998; Guéguen et al., 2005). The absorbance spectrum of ultrapure water blank (measured daily) was subtracted from samples' absorbance spectra.

2.5. Measurements of colloidal size spectra using FIFFF

The FIFFF system (Postnova F-1000) was coupled online with a UV-absorbance (Model 228, ISCO) and two fluorescence detectors (Waters Model 474 and LabAlliance Acufluor LC-305). The instrumental settings for the FIFFF are shown in Table 3. Chromophoric DOM was detected by measuring the UV-absorbance at 254 nm (UV₂₅₄), while humic-like and protein-like DOM were detected by measuring the fluorescence at Ex/Em wavelengths of 350/450 nm

Table 3
Instrument parameters for the analysis using flow field-flow fractionation.

nactionation.	
Parameter	Details or values
Accumulation wall membrane	1 kDa polyether sulfone
	(Omega, Pall Filtron)
Carrier solution	10 mM NaCl, 5 mM boric
	acid, $pH = 8$
Sample volume (ml)	10
On-line pre-concentration	
Channel flow rate (ml/min)	0.5
Focus flow rate (ml/min)	4.5
Focus (injection) time (min)	10
Relaxation	
Equilibration time (min)	1
Elution	
Channel flow rate (ml/min)	0.5
Cross flow rate (ml/min)	3.0
Run time (min)	60

 $(Fluo_{350/450})$ and 275/340 nm $(Fluo_{275/340})$, respectively. The analytical procedures and conditions are described elsewhere (Stolpe et al., 2010; Stolpe et al., 2014) and the choice of fluorescence settings was based on previous reports (Coble et al., 1990; Yamashita and Tanoue, 2003; Coble, 2007). Since the size of natural DOM is mostly <10 nm (Guo and Santschi, 2007), our focus in this study was mainly on the colloidal size <20 nm. Therefore, the flow settings of the FIFFF (Table 3) were optimized for determining the colloidal size spectrum with a high resolution in the 0.5–20 nm size range. At the end of separation $(\sim 60 \text{ min})$, the cross flow was turned off for the rapid elution and detection of the remaining colloidal materials in the >20 nm range. The conversion of FIFFF retention time to diffusion coefficient and hydrodynamic diameter was accomplished through calibration using proteins with known molecular weights and diffusion coefficients, including ovalbumin, bovine serum albumin, ferritin and thyroglobulin, under the same settings as sample analysis (Stolpe et al., 2010). Quinine sulfate standards were used to quantify fluorescent DOM based on calibration curves built from a series (4-5) of quinine sulfate standards using their integrated signals at Fluo_{350/450} (Coble et al., 1998; Stolpe et al., 2014). Thus, absorbance and fluorescence intensities are reported in ppb-quinine sulfate equivalents (ppb-OSE). Integrations of the full colloidal spectra (including the >20 nm material) were used to quantify the FIFFF-recoverable colloids and are denoted as [UV₂₅₄]_{FFF}, [Fluo_{350/450}]_{FFF} and [Fluo_{275/340}]_{FFF}. The colloidal size spectra were also integrated over smaller size ranges, such as the 0.5-4 nm, 4-20 nm and >20 nm, and the proportions of DOM in these size intervals were calculated as fractions relative to the whole FIFFF-recoverable fraction, for example, $[UV_{254}]_{0.5-4nm}/[UV_{254}]_{FFF}$.

2.6. Laboratory mixing experiment

Laboratory experiments were conducted to mimic the mixing between river water and seawater in the SLB estuary, in order to examine the dynamic change in colloidal size spectra as a result of estuarine mixing and resultant physicochemical processes. The end-member river water from the JR (S = 0.2) and seawater from the northern Gulf of Mexico (S = 30) were mixed in varying proportions to generate samples with different salinities (S = 0.2, 3, 6, 8, 10, 14, 18, 22, 26, and 30). The mixing samples were stored dark at 4 °C for 2 h and then were filtered through GF/F filters (0.7 µm) to remove materials that flocculated during mixing. The filtrates were measured for DOC concentrations, UV absorbance, and colloidal size spectra using FIFFF. Note that the DOC concentration of JR water for the mixing experiment was considerably lower than that during field gradient sampling and only physicochemical processes were being tracked in the short-term mixing experiment.

2.7. Data statistics

All statistical analyses were done in MATLAB 6.5.1 (Mathworks). One-way ANOVA tests were performed to

examine significance of differences of data between different sample sets.

2.8. Fluorescent DOM components from fluorescence excitation emission matrix analysis

The water samples used for FIFFF analysis were also measured for their fluorescent properties using fluorescence excitation emission matrices (EEMs). Detailed method description has been provided in Zhou et al. (2013). In summary, EEMs were first collected covering excitation and emission wavelength rages of 220–400 nm and 240–550 nm, respectively. Based on the EEM data, major DOM components were then derived using parallel factor (PARAFAC) analysis (Andersen and Bro, 2003; Stedmon and Bro, 2008). In addition, the biological index (BIX) was also determined from fluorescence EEMs as the ratio of emission between 380 and 430 nm under excitation at 310 nm and used as an index of autochthonous DOM (Huguet et al., 2009; Birdwell and Engel, 2010).

3. RESULTS

3.1. Characteristics of bulk DOM in river waters

Concentrations of DOC in the lower MR ranged from 236 to 343 μ M, with an average of 290 \pm 37 μ M (Table 1). The highest DOC concentration (343 μ M) was found at the highest river discharge (34,688 m³/s), although no significant correlation was found between DOC and discharge ($r^2 = 0.14$, p > 0.1). Compared to the lower MR, significantly higher DOC concentrations (p < 0.001) were found in the EPR, ranging from 326 to 1121 μ M, with an average of 645 \pm 230 μ M (Table 1). Overall, a significant correla-

tion was found between DOC in the EPR and discharge in the Pearl River at Bogalusa ($r^2 = 0.55$, p < 0.01).

Bulk colloidal organic carbon (COC) concentrations, as quantified by the ultrafiltration permeation model, ranged from 151 to 204 μM in the lower MR (average of 177 \pm 20 μM , Table 1), comprising 57–61% of the bulk DOC. Only one sample was collected in the EPR for ultrafiltration, which was during a flooding event, and the concentration of COC was 604 μM (Table 1), comprising 72% of the bulk DOC.

3.2. Colloidal size spectra in river waters

Examples of the colloidal size spectra of the chromophoric, humic-like, and protein-like DOM are shown in Fig. 2. Within the 0.5–20 nm hydrodynamic diameter (d_H) range, chromophoric (UV₂₅₄) and humic-like DOM (Fluo_{350/450}) both showed one narrow peak at 0.5-4 nm, centered at 1.5 ± 0.5 nm for chromophoric DOM and at 1.2 ± 0.5 nm for humic-like DOM (Fig. 2). In contrast, the colloidal size spectra of protein-like DOM (Fluo_{275/340}) showed multiple peaks. One peak at 0.5-4 nm matched the spectra of chromophoric and humic-like DOM, while an additional peak occurred at 3-8 nm, centered at 4.8 \pm 0.4 nm (Fig. 2). In addition, a high abundance of protein-like DOM was also detected in the >20 nm range (Fig. 2). The differences in colloidal size spectra of chromophoric, humic-like and protein-like DOM types indicate that distinct populations of colloids with different compositions occur in the samples.

To better quantify the partitioning of colloids between different size ranges, the colloidal size spectra were integrated over the intervals 0.5–4 nm, 4–20 nm and >20 nm, respectively. As shown in Fig. 3, more than 74% of the

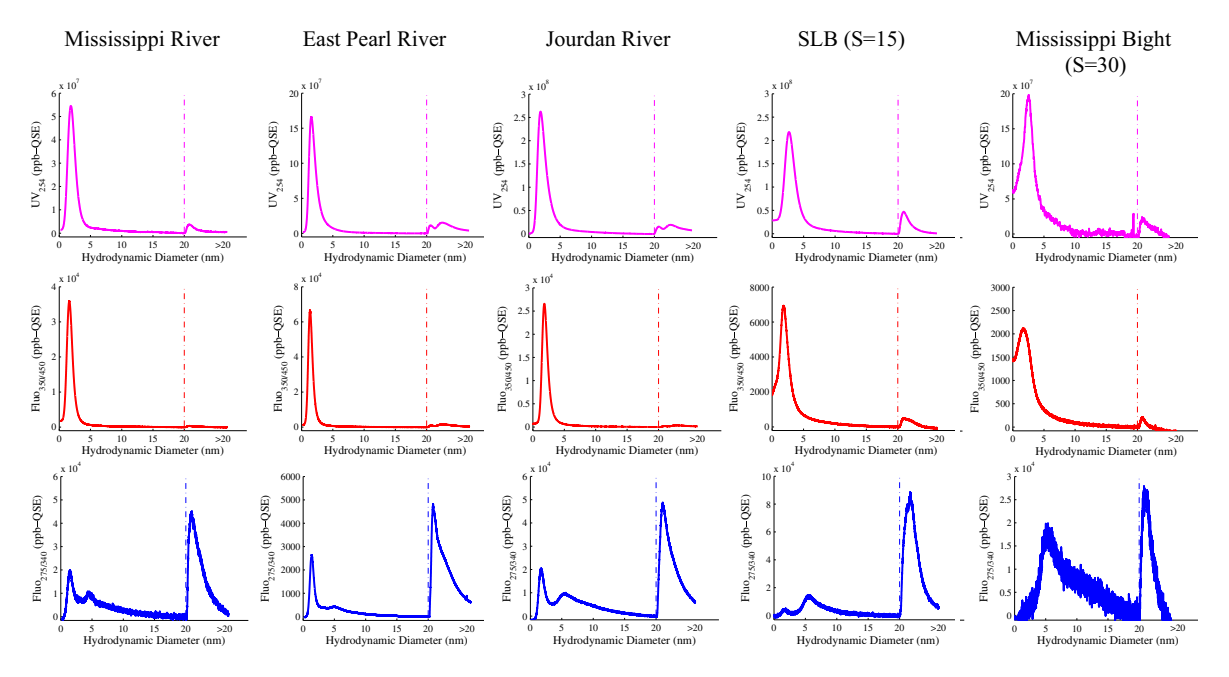
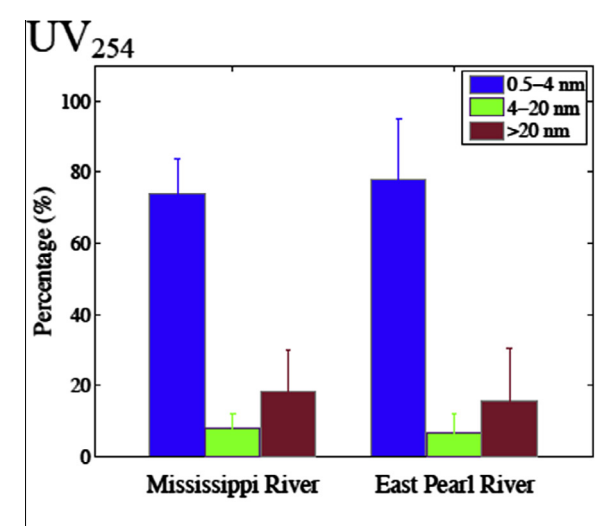
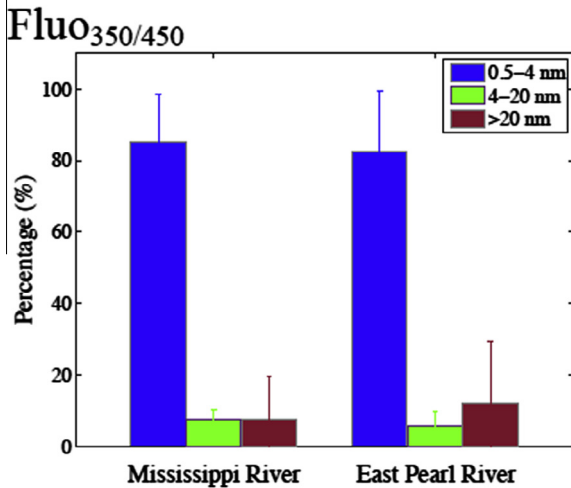


Fig. 2. Examples of colloidal size spectra of chromophoric (UV₂₅₄), humic-like (Fluo_{350/450}), and protein-like (Fluo_{275/340}) DOM in the lower Mississippi River (sample collected on November 30, 2009), the East Pearl River (December 28, 2009), the Jourdan River (Oct 15, 2009), St. Louis Bay (SLB) (Oct 15, 2009, S = 15), and Mississippi Bight (S = 30). The peak observed at >20 nm corresponds to all materials larger than 20 nm that eluted together after shutting down of cross flow.





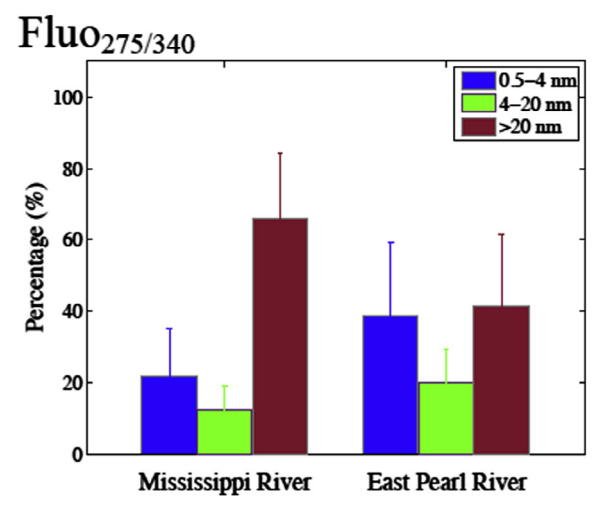


Fig. 3. Relative importance of colloidal chromophoric (top panel), humic-like (middle panel) and protein-like (bottom panel) DOM in the 0.5–4 nm, 4–20 nm and >20 nm size fractions, as compared with the total FIFFF-recoverable colloidal fraction, in the lower Mississippi River and the East Pearl River.

FIFFF-recoverable chromophoric DOM and more than 83% of the FIFFF-recoverable humic-like DOM were

found in the 0.5-4 nm size fraction in the lower MR and PR. In contrast, large fractions of the FIFFF-recoverable protein-like DOM (66% for the lower MR and 41% for the EPR) were found in the >20 nm size fraction (Fig. 3), again showing that protein-like DOM in river waters was mostly associated with large colloids. Note that the FIFFF-recoverable DOM in this study does not include the <1 kDa size fraction due to the pore-size (1 kDa) of the FIFFF channel membrane. Additional terrestrial and autochthonous DOM is likely to partition to the <1 kDa size fraction as well, but the reported size partitioning in this study only pertains to the recoverable colloidal (>1 kDa) size fraction.

3.3. Colloidal size distribution in estuarine waters

Along the river-seawater transect, concentrations of DOC decreased from 1618 µM in the JR to an average value of 972 μM in the SLB estuary, then to 234 μM in the MB (Table 2). As shown in Fig. 4, both DOC and UV-absorbance showed a conservative mixing behavior within the SLB estuary ($S \leq 15$). Beyond salinity 15 outside the SLB estuary, DOC showed a different mixing trend due to the influence of different coastal waters in the MS and MB (Blumberg et al., 2001; Wang et al., 2010). The concentrations of COC decreased from 1107 µM in the JR to 415 µM in SLB and 99 µM in the higher salinity waters, and also showed different mixing trends in the SLB estuary and the coastal waters (Table 2). The COC% in the bulk DOC also decreased along the salinity gradient from 68% in river water to 51% in estuarine and 42% in coastal waters (Table 2). The absorption coefficient at 254 nm (a₂₅₄) was positively correlated with DOC ($r^2 = 0.99$, p < 0.00001) and decreased with increasing salinity (Fig. 4), showing a major DOM source from river waters.

The abundance of colloidal chromophoric DOM quantified as [UV₂₅₄]_{FFF} decreased from 1934 ppb-QSE in the JR to an average of 380 ppb-QSE in SLB and to 26 ppb-OSE in the MB, showing an evident non-conservative mixing trend (Fig. 5). Similarly, the [UV₂₅₄]_{FFF}/COC ratio decreased from 1.67 g-QSE/mol-C in the JR to an average value of 0.67 g-QSE/mol-C in the SLB and then to 0.23 g-QSE/mol-C in the MB (Fig. S1). As shown in Fig. 5, the abundance of colloidal humic-like DOM quantified as [Fluo_{350/450}]_{EFF} decreased from 8.63 ppb-QSE in the JR to 2.51 ppb-QSE in SLB, and then to 0.08 ppb-OSE in the MB. In addition, the abundance of protein-like DOM quantified as [Fluo_{275/340}]_{FFF} generally decreased along the salinity gradient (Fig. 5). The ratio of colloidal protein-like to humic-like DOM ([Fluo_{275/340}]_{FFF}/ [Fluo_{350/450}]_{EFE}), on the other hand, increased from 1.4 in river water to 6.1 in estuarine waters and to 13.7 in coastal waters in the MB.

4. DISCUSSION

4.1. Factors affecting the abundance of bulk DOM and COM

No significant correlation was found between DOC concentration and discharge in the lower Mississippi River,

probably due to integration of signals from multiple tributaries and mixed DOM sources (Bianchi et al., 2004; Duan et al., 2007a; Wang et al., 2013; Cai et al., 2015). In contrast, DOC concentrations were significantly correlated with river discharge in the Pearl River, suggesting a hydrological control of the DOC-concentration relationship (Dalzell et al., 2007).

The higher COC concentration and colloidal fraction in the EPR are consistent with the higher forest coverage in the EPR drainage basin, with forest top soil contributing fresh HMW-DOM to the river (Mattsson et al., 2005). In contrast, the lower COC concentrations and colloidal fractions in the MR were probably due to the combined effects of agricultural land contributing more degraded LMW-DOM to the river (e.g., Cronan et al., 1999; Dalzell et al., 2011), levees restricting the inputs of terrestrial organic matter to the river, and intensive degradation (photochemically and/or biologically) of DOM during its long transport and residence time in dams and reservoirs (Duan et al., 2013).

Ultrafiltration is a physical size separation with minimal sample perturbation since no carrier solution or pH adjustment is needed. However, its results provide only the abundance of bulk colloidal size fraction larger than membrane's size cutoff (Guo and Santschi, 2007). In contrast, FIFFF offers continuous colloidal size separation and characterization (Zhou and Guo, 2015) although DOM conformation structure may be altered if the ionic strength and pH between the original sample and the carrier solution are different since usage of a carrier solution is necessary to minimize interactions between different analytes and between analytes and the FIFFF membrane (Giddings, 1993; Williams et al., 1997; Du and Schimpf, 2002). Thus, caution should be taken when comparing results between ultrafiltration and FIFFF analyses (see sections below). Nonetheless, the application of both techniques should provide new insights into understanding the DOM composition and size portioning in aquatic environments.

4.2. Factors affecting the colloidal size spectra of river and estuarine waters

It is likely that the small sized colloidal DOM at 0.5-4 nm was largely composed of fulvic acid, as suggested in previous studies (Beckett et al., 1987; Zanardi-Lamardo et al., 2002; Stolpe et al., 2014). The smaller sized humiclike DOM compared to chromophoric DOM is consistent with other studies, and suggests the existence of lightabsorbing moieties that either do not fluoresce or fluoresce less intensively at larger size fractions (Zanardi-Lamardo et al., 2002; Stolpe et al., 2010; Guéguen and Cuss, 2011). In contrast, the protein-like DOM in the 0.5-4 nm is associated with the same type of presumed fulvic acid as the humic-like DOM in this size range. For example, it has been found that phenol-like DOM can also fluoresce at the Ex/Em wavelengths of typical protein-like DOM (Maie et al., 2007; Hernes et al., 2009). It is also possible that the apparent protein-like DOM (detected at Ex/Em 275/340 nm) in the 0.5-4 nm size range is an interference from the emission peak of humic-like DOM extending to

the wavelength range of protein-like DOM (Stolpe et al., 2014). Additionally, previous studies showed terrestrial sources of colloidal amino acids in the lower Pearl River (Duan et al., 2007a). The protein-like colloids in the 3–8 nm and >20 nm size ranges are likely derived from *in situ* production since it has been shown that protein-like DOM in rivers is mainly derived from autochthonous sources, (Fellman et al., 2010; Williams et al., 2010) and freshly produced DOM is typically larger in size than more degraded and humic-like DOM (Amon and Benner, 1996).

Our results on the size partitioning of humic-like DOM are similar to those observed in other aquatic systems (Guéguen and Cuss, 2011). In addition, our finding that the >20 nm fraction comprised a larger portion of the protein-like DOM in the lower MR than in the EPR agrees with the higher autochthonous DOM production in the MR (Duan et al., 2007a; Cai et al., 2015) and the larger size of fresh autochthonous DOM as compared with more degraded DOM (Amon and Benner, 1996).

By integrating the whole colloidal size spectrum of chromophoric DOM, the abundance of FIFFF-recoverable colloidal chromophoric DOM ([UV₂₅₄]_{FFF}) can be calculated. Lower MR waters had [UV₂₅₄]_{FFF} values ranging from 36 ppb-QSE during low flow to 261 ppb-QSE during high flow (average of 137 ppb-QSE, Fig. S2). No significant correlation was found between [UV254]FFF and discharge $(r^2 < 0.01, p > 0.05, \text{ Fig. S2})$ or between $[UV_{254}]_{FFF}$ and DOC concentration ($r^2 < 0.05$, p > 0.1, Fig. S3) in the lower MR, indicating the lack of a simple hydrological control on colloidal chromophoric DOM and/or higher existence of non-chromophoric colloidal DOM in the river. Values of [UV₂₅₄]_{FFF} in the EPR ranged from 123 ppb-QSE during base flow to 4267 ppb-QSE during flood season, with an average of 1197 ppb-QSE (Figs. S3 and S4), which is considerably higher ($p \le 0.005$) than in the lower MR. The correlation between [UV₂₅₄]_{EFF} in the EPR and discharge in the Pearl River at Bogalusa ($r^2 = 0.71$, p < 0.002, Fig. S2) was stronger than the correlation between bulk DOC and discharge ($r^2 = 0.55$, p < 0.01). Thus, the input of colloidal chromophoric DOM to the river, and its contribution to the total DOC pool increased during high discharge probably as a result of increased soil leaching and surface water runoff. A stronger correlation between [UV254]FFF and DOC was found in the EPR ($r^2 = 0.43$) than in the lower MR ($r^2 = 0.05$, Fig. S3), indicating that the chromophoric colloidal component was more important in the EPR than in the lower MR. This observation can be explained by the higher forest coverage in the EPR drainage basin, with forest top soil contributing highly aromatic DOM to the river (Duan et al., 2007a).

The ratio between $[UV_{254}]_{FFF}$ and COC has been used as the counterpart to $SUVA_{254}$ (the ratio of UV absorbance to DOC concentration), representing aromaticity of colloidal organic matter (Weishaar et al., 2003; Stolpe et al., 2010), although their absolute values are not comparable. The $[UV_{254}]_{FFF}/COC$ ratio in the lower MR ranged from 0.18 to 1.00 g-QSE/mol-C with an average of 0.57 g-QSE/mol-C, and was 4.50 g-QSE/mol-C in the sample collected during a flood event (April 07, 2009) in the EPR. Considerably higher $[UV_{254}]_{FFF}/COC$ ratio in the EPR indicates

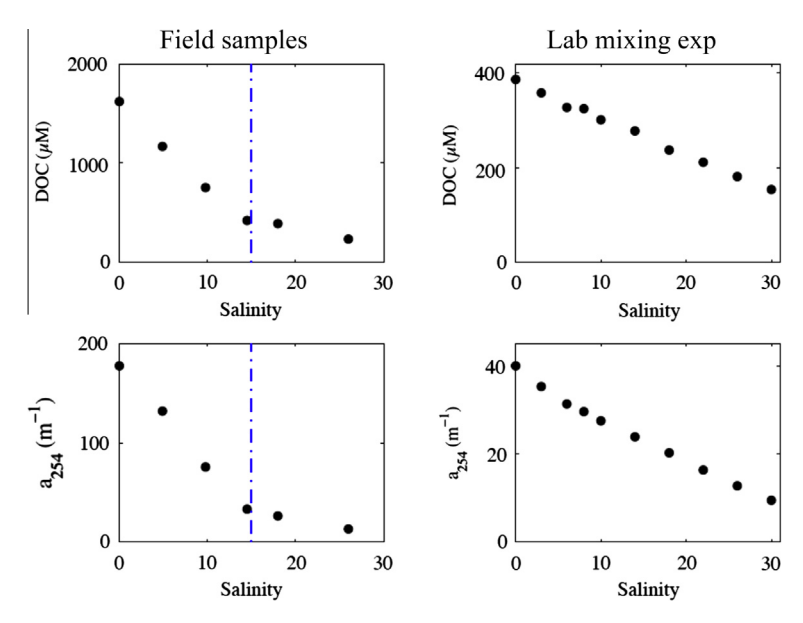


Fig. 4. Variations of DOC (upper panels) and UV-absorbance at 254 nm, a_{254} (lower panels) along the river-sea water transect in field samples (left panels) and samples from the laboratory mixing experiment (right panels). Note that in the plots for the field samples, dotted lines were marked at salinity = 15, corresponding to the salinity at the mouth of St. Louis Bay, to help visualize different DOM characteristics inside and outside the Bay.

greater aromaticity of colloidal DOM in the EPR than the MR, which is consistent with the higher importance of lignin-phenols, an aromatic biomarker for terrestrial organic matter, in the EPR compared to the MR (DUAN et al., 2007a).

The proportion of colloidal humic-like DOM in the bulk DOM was quantified by the ratio of [Fluo_{350/450}]_{FFF} to the bulk DOC. In the lower MR, the [Fluo_{350/450}]_{FFF}/DOC ratio ranged from 0.00012 to 0.010 g-QSE/mol-C with an average of 0.0049 g-QSE/mol-C (Fig. S3). Similar to the bulk DOC and other colloidal components, no significant correlation with discharge was found for [Fluo_{350/450}]_{FFF}, possibly due to diverse sources and multiple controlling factors of humic-like colloidal DOM in the MR basin. In the EPR, the [Fluo_{350/450}]_{FFF}/DOC ratio ranged from 0.0022 to 0.039 g-QSE/mol-C (averaging 0.014 g-QSE/mol-C), which was significantly greater than that in the lower MR (p < 0.01). In addition, [Fluo_{350/450}]_{FFF}/DOC was significantly correlated with discharge in the PR ($r^2 = 0.43$, p < 0.01), suggesting increased importance of humic substances in the bulk DOM pool with increasing discharge in the PR.

The relative importance of colloidal protein-like DOM in comparison with colloidal chromophoric DOM can be evaluated by the ratio of [Fluo_{275/340}]_{FFF} to [UV₂₅₄]_{FFF} (Fig. S3). Samples from the lower MR had [Fluo_{275/340}]_{FFF} /[UV₂₅₄]_{FFF} ratios ranging from 0.011 to 0.090 (averaging 0.035), while samples from the EPR had [Fluo_{275/340}]_{FFF} /[UV₂₅₄]_{FFF} ratios ranging from 0.0024 to 0.048 (averaging 0.013). Significantly lower [Fluo_{275/340}]_{FFF} /[UV₂₅₄]_{FFF} ratios in the EPR (p < 0.005) point to a compositional difference between lower MR and EPR waters, with more *in situ* biological production and thus more protein-like colloidal DOM in lower MR waters, and more soil-derived

humic-like DOM from the EPR. This is consistent with previous observations using other techniques and/or biomarkers for the lower MR and EPR (Duan et al., 2007a, 2013). Interestingly, the [Fluo_{275/340}]_{FFF}/[UV₂₅₄]_{FFF} ratio exhibited a negative correlation with discharge in the MR ($r^2 = 0.59$, p < 0.005,), but showed no correlation with discharge in the EPR. The decrease in [Fluo_{275/340}]_{FFF}/[UV₂₅₄]_{FFF} ratio with increasing discharge in the lower MR suggests different sources of colloidal chromophoric and protein-like DOM. As previously hypothesized, a major source of colloidal chromophoric DOM was from the leaching of soil and plant litter during high flow, while colloidal protein-like DOM was mostly autochthonous in nature and subject to dilution during high flow.

Correlations were found between DOM components at specific size ranges derived from FIFFF and fluorescent DOM components derived from fluorescence EEMs and PARAFAC analysis. As shown in Fig. S4, representative fluorescent DOM components identified from EEMs in the two rivers (detected and modeled from the same water samples for FIFFF analysis) include a humic-like (Component-1, C1, upper panel) and a protein-like (Component-6, C6, lower panel) component. The proportion of humic-like DOM found in the 0.5-4 nm size fraction can be expressed as the [Fluo_{350/450}]_{0.5-5nm-FFF}/DOC ratio, and was positively correlated to the percentage of fluorescent DOM associated with C1 (C1%) in both MR $(r^2 = 0.49, p < 0.01)$ and EPR waters $(r^2 = 0.33, p = 0.05)$. This suggests that the 0.5-4 nm humic-like colloids represent a considerable portion of C1 and/or exhibited similar behavior as C1. In the MR, the relative importance protein-like DOM in the >20 nm $([Fluo_{275/340}]_{\geq 20nm\text{-}FFF}/DOC)$ was positively correlated $(r^2 = 0.45, P = 0.01)$ with the percentage of fluorescent

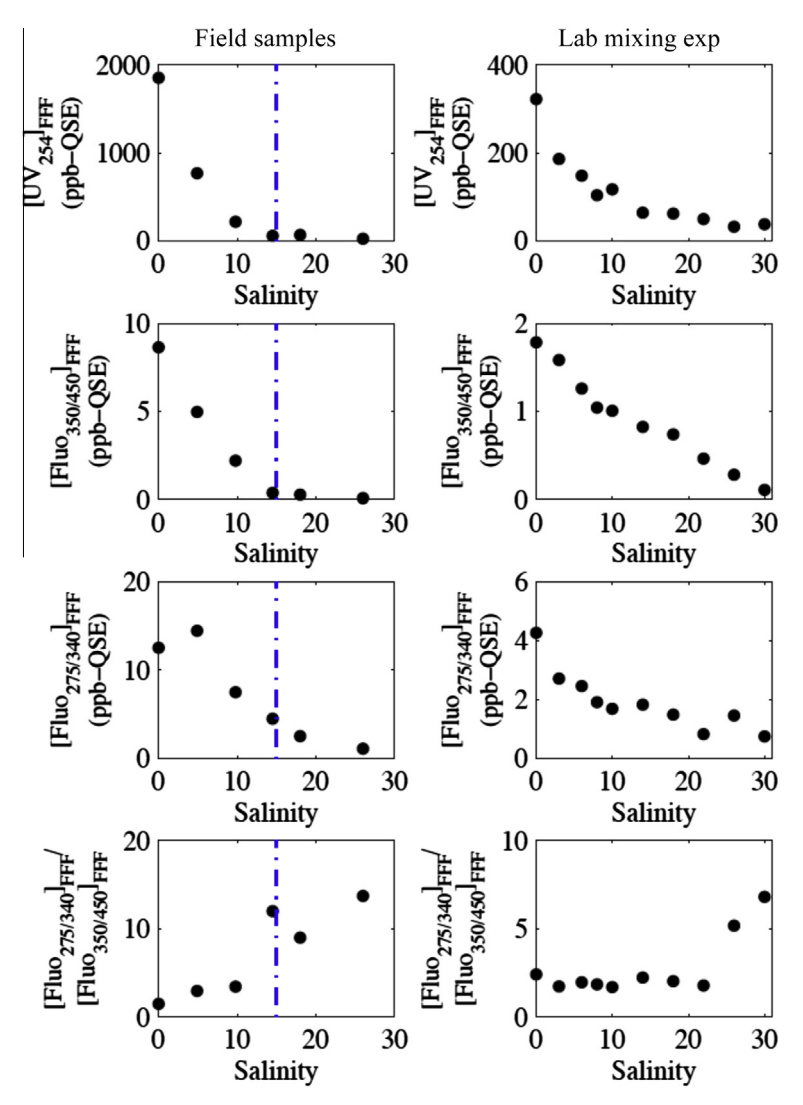


Fig. 5. Variations of $[UV_{254}]_{FFF}$ (ppb-QSE), $[Fluo_{350/450}]_{FFF}$ (ppb-QSE), $[Fluo_{275/340}]_{FFF}$ (ppb-QSE), and $[Fluo_{275/340}]_{FFF}$ (ppb-QSE), and in samples from the laboratory mixing experiment (right panels). Again, the dotted lines at S=15 in the plots for field samples help visualize different colloidal DOM mixing behavior inside and outside the bay.

DOM associated with C6 (C6%) (Fig. S5). Again, this further suggests the protein-like C6 mostly partitioned to larger (>20 nm) size ranges and/or behaved similarly as larger-sized protein-like DOM in the MR. In the EPR, no correlation was found between [Fluo_{275/340}]>20nm-FFF/DOC and C6% ($r^2 = 0.02$, p = 0.63), likely due to lesser degree of DOM reworking and lower existence of protein-like DOM compared with the lower MR. The correlation between results found in FIFFF and fluorescence EEM analyses shows compatibility and confirmation of the findings from the two methods, and provides new insights into the composition and size distribution of DOM in natural waters.

The colloidal size spectra of chromophoric and humiclike DOM in the JR and the SLB estuary showed a major narrow peak at 0.5–4 nm, similar to the observations in the MR and EPR samples (Fig. 2). It is likely that the chromophoric and humic-like colloidal DOM in the SLB estuary was associated with the same type of presumed fulvic

acid colloids as in the rivers. Integration of the colloidal size spectra over different size ranges showed that proportion of the FIFFF-recoverable humic-like DOM in the 0.5-4 nm size fraction decreased from 89% in the JR to an average value of 83% in SLB and to 72% in the MB (Fig. 6), suggesting a slight shift in the size of colloidal humic substances from small to large sizes as the salinity increased. The colloidal size spectra of protein-like DOM showed two peaks in the 0.5-4 nm and 3-8 nm size ranges, but the major portion of the colloidal protein-like DOM was associated with the >20 nm materials (Fig. 2). The percentage of the FlFFF-recoverable protein-like DOM found in the >20 nm size fraction increased from 60% in the JR, to 61% in SLB, and \sim 71% in the MB (Fig. 6), showing increased importance of large-sized protein-like colloids in coastal waters. This observation agrees well with our hypothesis that the medium and large sized protein-like colloids are formed by in situ production. In addition, the

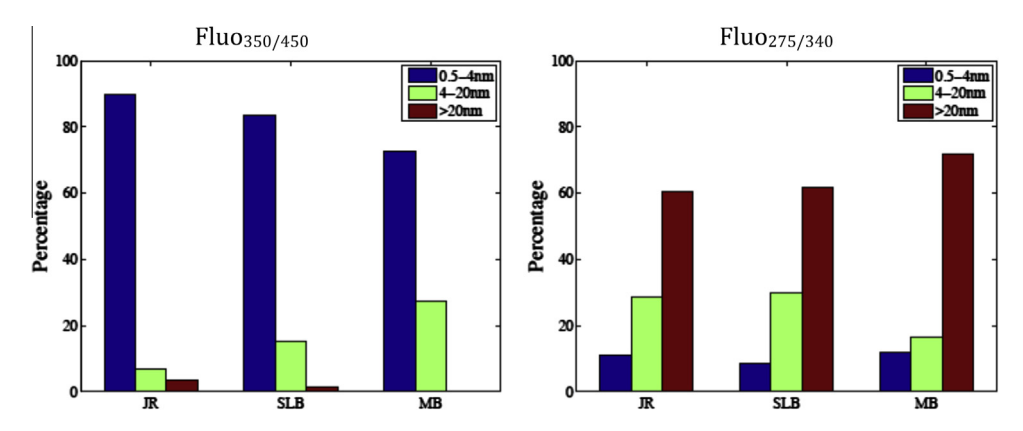


Fig. 6. Relative importance of colloidal humic-like (Fluo_{350/450}, left panel) and protein-like (Fluo_{275/340}, right panel) DOM in the 0.5–4 nm, 4–20 nm and \geq 20 nm size fractions, as calculated by their fractions in the FIFFF-recoverable colloidal size range, from the Jourdan River (JR), St. Louis Bay (SLB) estuary, and the Mississippi Bight (MB).

>20 nm colloids could be formed through the flocculation of smaller colloids during estuarine mixing (Sholkovitz, 1976) (see also discussion below).

The decrease in the abundance of colloidal chromophoric DOM and the $[UV_{254}]_{EFF}/COC$ ratio with salinity indicate a decrease in the abundance and loss in aromaticity of colloidal DOM from river to estuary and to coastal waters. Fig. 5 shows that the abundance of protein-like colloidal DOM decreased by a slower rate than humic-like colloidal DOM going from river water to coastal seawater, and is likely the result of an additional source of protein-like DOM from marine production. There is a seeming deviation from the general increasing trend at mid-salinity (S \sim 15), where [Fluo_{275/340}]_{FFF}/[Fluo_{350/450}]_{FFF} ratio is higher than what would be expected based on the trend observed at all the other stations. Fluorescence EEM results show that a similar positive deviation of the biological index (BIX), an index representing autochthonous sources, was also observed at this station (Fig. S6), indicating a higher proportion of autochthonous DOM at this mid-salinity station. Additionally, the highest chlorophyll-a concentration was found in the same region in the MS at this season (Stolpe et al., 2014). Thus, the high ratio between protein-like and humic-like DOM observed at mid- and higher-salinity stations in the study area was probably a result of high in situ DOM production.

4.3. Mixing behavior of different sized colloidal DOM in estuarine waters

The mixing behavior of DOC has been widely reported in Gulf of Mexico estuaries, showing conservative, addition, or removal behavior (Guo and Santschi, 1997b; Guo et al., 1999; Wang et al., 2010). Nevertheless, to the best of our knowledge, there are no studies reporting the estuarine mixing behavior of colloids in different sizes incorporating both field studies and laboratory mixing experiments. As shown in Fig. 4 for the bulk DOC and a₂₅₄ in the field samples, there was an apparent DOC removal over the entire salinity range, from the JR to SLB and extending to MS and MB. However, a closer look at these data reveals

that within the SLB estuary (salinity \leq 15), the bulk DOC actually had a conservative mixing behavior (Fig. 4). As pointed out by Wang et al. (2010), the apparent removal of bulk DOC in the waters outside SLB is largely due to the occurrence of different coastal waters with different DOC endmember concentrations, resulting in a two-segment mixing trend.

In contrast to the conservative mixing observed for the bulk DOC, the colloidal chromophoric DOM ([UV₂₅₄]_{FFF}) indeed showed significant removal within the SLB estuary (Fig. 5). Chromophoric DOM in the 0.5–4 nm size fraction ([UV₂₅₄]_{0.5–4nm}) also showed the same trend as [UV₂₅₄]_{FFF} or the bulk colloidal chromophoric DOM in the field samples (Fig. 7), since most of the FIFFF-recoverable chromophoric DOM partitioned to the 0.5–4 nm size range (Section 3.3). However, similar to the bulk DOC, the colloidal humic-like DOM ([Fluo_{350/450}]_{FFF}) and humic-like DOM in the 0.5–4 nm size range ([Fluo_{350/450}]_{0.5–4nm}) seemed to exhibit conservative behavior within SLB with a salinity <15 (Figs. 5 and 7), showing distinct estuarine mixing behavior among colloids with different composition and sizes.

Similar to the field data, laboratory mixing experiments using end-member river water (DOC: 387 µM; [UV₂₅₄]_{FFF}: 321 ppb-QSE) and seawater (S = 30; DOC: 154 μ M; [UV₂₅₄]_{FFF}: 37 ppb-QSE) also showed conservative mixing behaviors of DOC and a₂₅₄ values (Fig. 4), but a removal of [UV₂₅₄]_{FFF} and [UV₂₅₄]_{0.5-4nm} with increasing salinity (Figs. 5 and 7). Also similar to the field data, the humiclike DOM in both the bulk colloidal ([Fluo_{350/450}]_{FFF}) and the 0.5-4 nm size fraction ([Fluo_{350/450}]_{0.5-4nm}) demonstrated an overall conservative mixing behavior (Figs. 5 and 7). Similar results observed between field data and laboratory mixing experiments suggest that physicochemical processes, such as sea salt-induced flocculation/coagulation, play the major role in regulating the mixing behavior of DOC and colloidal DOM in the estuary since the shortterm laboratory mixing experiment (2 h) likely excluded biological effects. Note that the JR sampling for the mixing experiment was carried out at a different time from that of the field study due to the labor-intensive nature for both

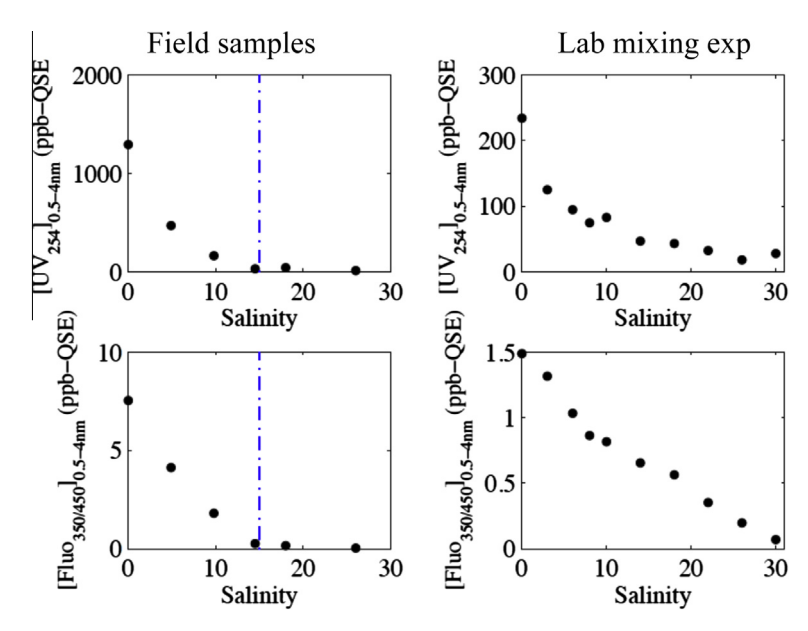


Fig. 7. Variations of $[UV_{254}]_{0.5-4nm}$ (ppb-QSE) and $[Fluo_{350/450}]_{0.5-4nm}$ (ppb-QSE) along the salinity gradient in field samples (left panels) and in the laboratory mixing experiment (right panels). The dotted lines at S=15 were also added.

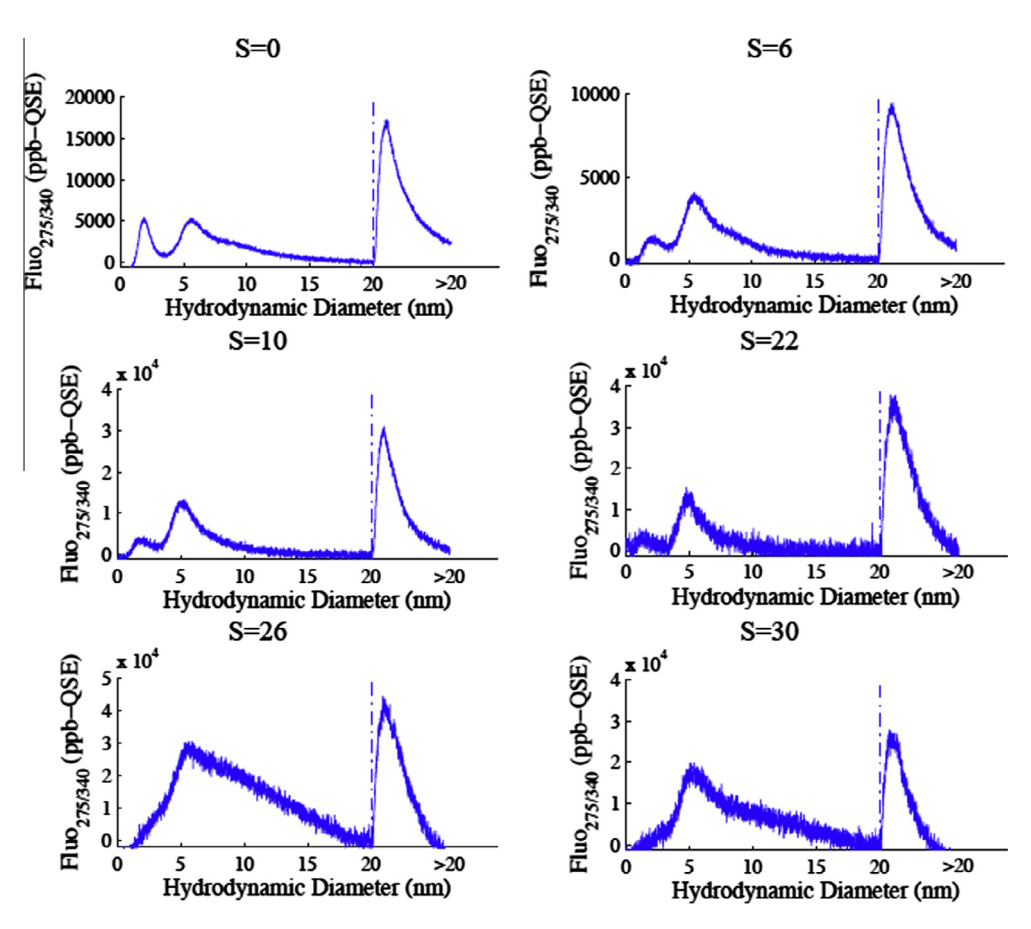


Fig. 8. Change in colloidal size spectra of protein-like DOM (Fluo_{275/340}) during the estuarine mixing experiment using end-member river water and seawater. A total of six examples are shown in the order of increasing salinity.

FIFFF analysis and ultrafiltration and the necessity to keep the samples fresh and measured as soon as possible. Unfortunately, DOC concentrations between the two sampling trips differed considerably. It is thus possible that the specific behavior of colloidal DOM in the mixing experiment was not exactly the same as that observed during field study. However, although DOC concentrations in the Jourdan River, a small forested river, were considerably different between the field study (1618 $\mu mol/L$) and the laboratory mixing experiment (387 $\mu mol/L$), the DOM composition can be expected to be similar and the behavior of the DOM during estuarine mixing should be comparable.

As shown in Fig. 8, the colloidal protein-like DOM (Fluo_{275/340}) in samples from laboratory mixing experiments was mostly partitioned to the >20 nm size fraction with a bi-modal size distribution in the low nm size range. The relative importance of the mid-size colloids (4–8 nm) as compared to the small size colloids (0.5–4 nm) increased with salinity (Fig. 8). In the end-member coastal seawater (S = 30) and high salinity mixed sample (e.g., S = 26), the size spectra of protein-like DOM in the low nanometer size range did not show a distinct bi-modal distribution (Fig. 8). Instead, they were characterized by one very wide peak from 0.5 to 15 nm (centered at 5–7 nm), reflecting a change in relative importance of protein-like DOM in different colloidal sizes from river to coastal waters (Fig. 9).

Integration of the colloidal size ranges showed that the abundance of protein-like DOM in small, mid- and large size fractions all decreased as salinity increased in the mixing experiment (Fig. 9). The small-sized protein-like DOM ([Fluo_{275/340}]_{0.5-4nm}) showed an apparent removal pattern (Fig. 9), similar to that of chromophoric DOM in this size range. As opposed to the small size colloids, the mid-sized protein-like DOM ([Fluo_{275/340}]_{4-8nm}) seemed to behave conservatively, especially in the low salinity range (Fig. 9). The wide peak of protein-like DOM in the low nanometer size range at high salinity as described above (Fig. 8) led to difficulties in a clear-cut separation of the small and mid-sized protein-like DOM and may have resulted in the scattered relationship of [Fluo_{275/340}]_{4-8nm} with salinity in the higher salinity range. The >20 nm protein-like DOM ([Fluo_{275/340}]>_{20nm}) showed removal behavior at low salinity during mixing (Fig. 9). It thus appears that the mid-sized protein-like DOM did not undergo significant flocculation while the small and large size fractions were affected by salt-induced flocculation. Both the ratio of $[Fluo_{275/340}]_{4-8nm}/[Fluo_{275/340}]_{0.5-4nm}$ $[Fluo_{275/340}]_{>20nm}/[Fluo_{275/340}]_{0.5-4nm}$ and ratio of increased with increasing salinity (Fig. 10, right panels), possibly linked to the transformation from small colloids to mid-sized colloids and large size colloids during estuarine mixing. However, this trend was less obvious in the field samples (Fig. 10, left panels). Highest [Fluo_{275/340}]_{4-8nm}/[Fluo_{275/340}]_{0.5-4nm} ratio was found at 15, salinity corresponding to relatively [Fluo_{275/340}]_{FFF}/[Fluo_{350/450}]_{FFF} ratio and BIX (Figs. 5 and S6), suggesting a source from freshly produced marine DOM. Previous work using size exclusion chromatography also separated protein-like DOM in the nanometer

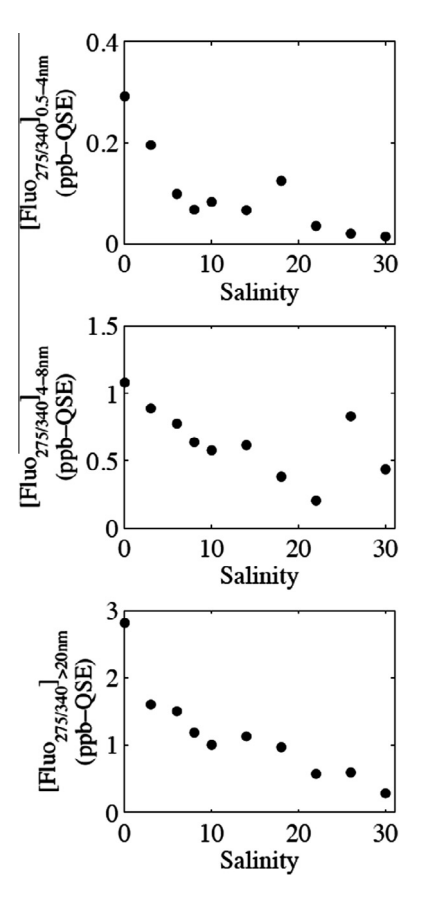


Fig. 9. Variations in colloidal protein-like DOM in the small size ([Fluo $_{275/340}$]_{0.5-4nm} (ppb-QSE), upper panel), mid size ([Fluo $_{275/340}$]_{4-8nm} (ppb-QSE), middle panel), and large size fraction ([Fluo $_{275/340}$]_{5-20nm} (ppb-QSE), lower panel) during the laboratory mixing experiment.

size range into two fractions and related the smaller one (~7 kDa, ~2.5 nm) with phenolic moieties of humic substances and the larger one (~50 kDa, ~4.5 nm) with proteinaceous DOM (Maie et al., 2007). Similarly, Maie et al. (2007) observed the ratio of 50 kDa to 7 kDa DOM fractions to be higher in coastal water of Florida Bay than in riverine/estuarine waters. DOM in different size fractions was clearly associated with distinct types of moieties. As shown in Fig. 10, the ratio of [Fluo_{275/340}]_{20nm}/[Fluo_{275/340}]_{0.5-4nm} also had its highest value at salinity ~15, suggesting autochthonous sources of the large size (>20 nm) protein-like DOM in this region.

Overall, the colloidal DOM size distributions measured in the laboratory mixing experiments resembled those observed in the natural estuarine samples. For example, chromophoric DOM showed removal in both the field study and laboratory mixing experiments, while humic-like DOM was more conservative inside the SLB and during laboratory mixing (Fig. 7). Physical mixing and salt-induced flocculation thus played an important role in governing the fate and transport of colloidal DOM in the estuary. Protein-like DOM, on the other hand, was characterized as autochthonous source in the 4–8 nm and >20 nm size intervals.

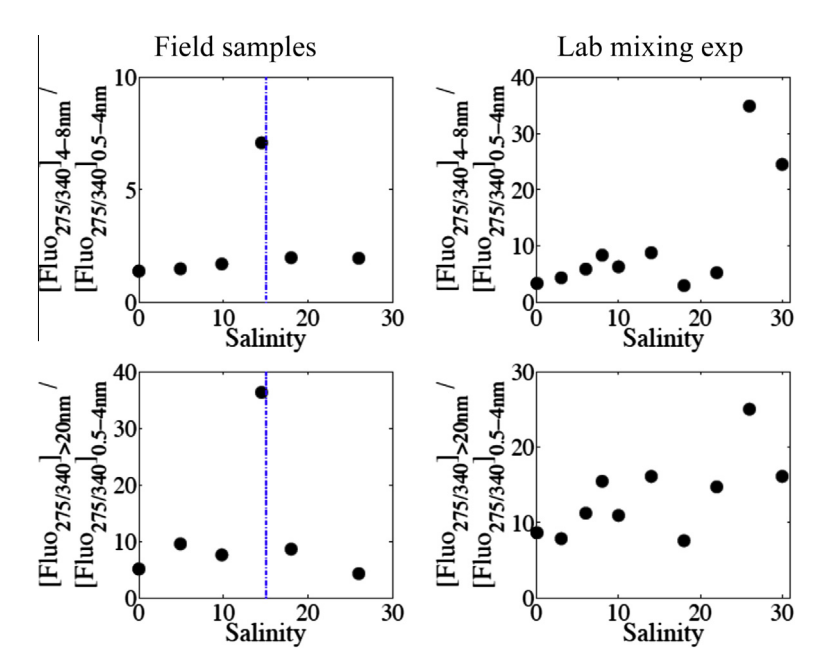


Fig. 10. Comparisons of the ratio of mid- to small sized colloidal protein-like DOM ($[Fluo_{275/340}]_{4-8nm}/[Fluo_{275/340}]_{0.5-4nm}$, upper panels) and the ratio of large to small sized protein-like DOM ($[Fluo_{275/340}]_{20nm}/[Fluo_{275/340}]_{0.5-4nm}$, lower panels) between field data (left panels) and laboratory mixing experiment (right panels). The dotted lines at S=15 were also marked.

5. CONCLUSIONS

Dissolved organic matter in the lower MR was characterized by its low abundance, low aromaticity and weak correlations with discharge, resulting from diverse DOM sources from tributaries in the river basin, degradation and modification of DOM during transport, and autochthonous sources from in situ production. Seasonal variations of colloidal DOM in the lower MR featured a decrease in the ratio of protein-like DOM to chromophoric DOM with increasing discharge, suggesting autochthonous sources of protein-like DOM that were subject to dilution during high flow. More optically active DOM was found in the large sized fractions (>20 nm) in the lower MR, compared to the EPR, where higher abundances of bulk DOM and humiclike DOM were observed, the latter of which occurred mostly in the <4 nm size fraction. These observations are consistent with the longer residence time and higher in situ production in the lower MR, and the difference in the sources of colloidal DOM is coherent with the drainage basin size, land use, and human influences on the two rivers.

In the SLB estuary, the abundance, aromaticity and relative importance of humic-like colloidal DOM decreased with salinity. However, the ratio of protein-like to humic-like colloidal DOM increased with increasing salinity, suggesting addition of autochthonous DOM and/or removal of humic-like DOM during estuarine mixing. Consistent with field observations, results from a laboratory mixing experiment clearly showed removal of the small sized colloidal chromophoric and fluorescent DOM, indicating salt-induced flocculation/coagulation during estuarine mixing in the SLB estuary. Most importantly, colloids with different sizes and composition exhibited different behaviors during estuarine mixing, with dynamic transformation between different size fractions in the estuary.

Two major types of colloids seemed to be present in coastal seawater. One type had a narrow peak at 0.5–4 nm in size showing chromophoric and fluorescent properties and was likely composed of natural fulvic acids. The other type of colloids were protein-like DOM with a larger size in the 4-8 nm and >20 nm ranges, mostly derived from *in situ* biological production. Different colloidal components exhibited distinct size spectra or size distributions. Therefore, colloidal size distributions of specific types of DOM characterized by the flow field-flow fractionation technique should provide new insights into better understanding of the transport and cycling pathways of natural organic matter in river, estuarine and coastal waters.

ACKNOWLEDGMENTS

We would like to thank Kevin Martin, Xuri Wang, and Peng Lin for their assistance during sample collection. We also thank Associate Editor, Thomas Bianchi, and three anonymous reviewers for their constructive comments which improved the manuscript. This work was supported in part by funding from NOAA through the Northern Gulf Institute (Projects #09-NGI-04 and 09-NGI-13), the National Science Foundation (OCE#0850957 and OCE-MRI#1233192), and the University of Wisconsin-Milwaukee (RGI).

APPENDIX A. SUPPLEMENTARY DATA

Supplementary data associated with this article can be found, in the online version, at http://dx.doi.org/10.1016/j.gca.2016.02.032.

REFERENCES

Aiken G. R., Hsu-Kim H. and Ryan J. N. (2011) Influence of dissolved organic matter on the environmental fate of metals,

- nanoparticles, and colloids. *Environ. Sci. Technol.* **45**, 3196–3201. http://dx.doi.org/10.1021/es103992s.
- Amon R. M. W. and Benner R. (1996) Bacterial utilization of different size classes of dissolved organic matter. *Limnol. Oceanogr.* 41, 41–51.
- Andersen C. M. and Bro R. (2003) Practical aspects of PARAFAC modeling of fluorescence excitation-emission data. *J. Chemom.* 17, 200–215. http://dx.doi.org/10.1002/cem.790.
- Baalousha M., Stolpe B. and Lead J. R. (2011) Flow field-flow fractionation for the analysis and characterization of natural colloids and manufactured nanoparticles in environmental systems: a critical review. J. Chromatogr. A 1218, 4078–4103.
- Bauer J. E., Cai W.-J., Raymond P. A., Bianchi T. S., Hopkinson C. S. and Regnier P. A. G. (2013) The changing carbon cycle of the coastal ocean. *Nature* 504, 61–70.
- Beckett D. C. and Pennington C. H. (1986) Water Quality, Macroinvertebrates, Larval Fishes, and Fishes of the Lower Mississippi River – A Synthesis. Waterways Experiment Station, Vicksburg, MS.
- Beckett R., Jue Z. and Giddings J. C. (1987) Determination of molecular weight distributions of fulvic and humic acids using flow field-flow fractionation. *Environ. Sci. Technol.* 21, 289–295.
- Benedetti M. F., Mounier S., Filizola N., Benaim J. and Seyler P. (2003) Carbon and metal concentrations, size distributions and fluxes in major rivers of the Amazon basin. *Hydrol. Process.* 17, 1363–1377.
- Benner R. and Amon R. M. W. (2015) The size-reactivity continuum of major bioelements in the ocean. *Ann. Rev. Mar. Sci.* 7. http://dx.doi.org/10.1146/annurev-marine-010213-135126.
- Bianchi T. (2007) *Biogeochemistry of Estuaries*. Oxford University Press, New York.
- Bianchi T. S., Filley T., Dria K. and Hatcher P. G. (2004) Temporal variability in sources of dissolved organic carbon in the lower Mississippi river. *Geochim. Cosmochim. Acta* 68, 959–967.
- Birdwell J. E. and Engel A. S. (2010) Characterization of dissolved organic matter in cave and spring waters using UV, ÄìVis absorbance and fluorescence spectroscopy. *Org. Geochem.* 41, 270–280.
- Blumberg A. F., Ahsan Q., Li H., Kaluarachchi I. D. and Lewis J. K. (2001). Circulation, sediment and water quality modeling in the Northern Gulf of Mexico. In *Proceedings of World Water and Environmental Resources Congress*, ASCE, May 20–24, Orlando, Florida.
- Boesch D. F., Boynton W. R., Crowder L. B., Diaz R. J., Howarth R. W., Mee L. D., Nixon S. W., Rabalais N. N., Rosenberg R., Sanders J. G., Scavia D. and Turner R. E. (2009) Nutrient enrichment drives gulf of Mexico hypoxia. *Eos Trans. AGU* 90, 117–118.
- Brunner C. A., Beall J. M., Bentley S. J. and Furukawa Y. (2006) Hypoxia hotspots in the Mississippi Bight. *J. Foraminiferal Res.* 36, 95–107.
- Cai Y. and Guo L. (2009) Abundance and variation of colloidal organic phosphorus in riverine, estuarine, and coastal waters in the northern Gulf of Mexico. *Limnol. Oceanogr.* 54, 1393–1402. http://dx.doi.org/10.4319/lo.2009.54.4.1393.
- Cai Y., Guo L., Wang X., Mojzis A. K. and Redalje D. G. (2012) The source and distribution of dissolved and particulate organic matter in the Bay of St. Louis, northern Gulf of Mexico. *Estuar. Coast. Shelf Sci.* 96, 96–104. http://dx.doi.org/10.1016/j.ecss.2011.10.017.
- Cai Y., Guo L., Wang X. and Aiken G. (2015) Abundance, stable isotopic composition, and export fluxes of DOC, POC, and DIC from the Lower Mississippi River during 2006–2008. J.

- Geophys. Res. Biogeosci. 120, 2273–2288. http://dx.doi.org/10.1002/2015JG003139.
- Chigbu P., Gordon S. and Strange T. R. (2005) Fecal coliform bacteria disappearance rates in a north-central Gulf of Mexico estuary. *Estuar. Coast. Shelf Sci.* 65, 309–318.
- Coble P. G. (2007) Marine optical biogeochemistry: the chemistry of ocean color. Chem. Rev. 107, 402–418.
- Coble P. G., Del Castillo C. E. and Avril B. (1998) Distribution and optical properties of CDOM in the Arabian Sea during the 1995 Southwest Monsoon. *Deep Sea Res. Part II* 45, 2195– 2223. http://dx.doi.org/10.1016/s0967-0645(98)00068-x.
- Coble P. G., Green S. A., Blough N. V. and Gagosian R. B. (1990) Characterization of dissolved organic matter in the Black Sea by fluorescence spectroscopy. *Nature* 348, 432–435.
- Cronan C. S., Piampiano J. T. and Patterson H. H. (1999) Influence of land use and hydrology on exports of carbon and nitrogen in a Maine river basin. J. Environ. Qual. 28, 953–961.
- Dalzell B. J., Filley T. R. and Harbor J. M. (2007) The role of hydrology in annual organic carbon loads and terrestrial organic matter export from a midwestern agricultural watershed. *Geochim. Cosmochim. Acta* 71, 1448–1462.
- Dalzell B. J., King J. Y., Mulla D. J., Finlay J. C. and Sands G. R. (2011) Influence of subsurface drainage on quantity and quality of dissolved organic matter export from agricultural landscapes. J. Geophys. Res. 116, G02023.
- Du Q. and Schimpf M. E. (2002) Correction for particle-wall interactions in the separation of colloids by flow field-flow fractionation. *Anal. Chem.* 74, 2478–2485.
- Duan S. and Bianchi T. (2006) Seasonal changes in the abundance and composition of plant pigments in particulate organic carbon in the lower Mississippi and Pearl Rivers. *Estuaries Coasts* 29, 427–442.
- Duan S., Bianchi T. S. and Sampere T. P. (2007a) Temporal variability in the composition and abundance of terrestriallyderived dissolved organic matter in the lower Mississippi and Pearl Rivers. *Mar. Chem.* 103, 172–184. http://dx.doi.org/ 10.1016/j.marchem.2006.07.003.
- Duan S., Bianchi T. S., Shiller A. M., Dria K., Hatcher P. G. and Carman K. R. (2007b) Variability in the bulk composition and abundance of dissolved organic matter in the lower Mississippi and Pearl rivers. J. Geophys. Res. 112, G02024. http://dx.doi. org/10.1029/2006JG000206.
- Duan S., Allison M. A., Bianchi T. S., McKee B. A., Shiller A. M., Guo L. and Rosenheim B. (2013) Transport and biogeochemical cycles of organic carbon and nutrients in the lower Mississippi River. In Biogeochemical Dynamics at Major River-Coastal Interfaces: Linkages with Global Change (eds. T. S. Bianchi, M. A. Allison and W.-J. Cai). Cambridge University Press, New York, USA.
- Fellman J. B., Hood E. and Spencer R. G. M. (2010) Fluorescence spectroscopy opens new windows into dissolved organic matter dynamics in freshwater ecosystems: a review. *Limnol. Oceanogr.* 55, 2452–2462.
- Giddings J. C. (1993) Field-flow fractionation: analysis of macromolecular, colloidal, and particulate materials. *Science* 260, 1456–1465.
- Goolsby D. A. and Battaglin W. A. (2001) Long-term changes in concentrations and flux of nitrogen in the Mississippi River Basin, USA. *Hydrol. Process.* 15, 1209–1226. http://dx.doi.org/ 10.1002/hyp.210.
- Goolsby D. A., Battaglin W. A., Aulenbach B. T. and Hooper R. P. (2000) Nitrogen flux and sources in the Mississippi River Basin. Sci. Total Environ. 248, 75–86. http://dx.doi.org/10.1016/s0048-9697(99)00532-x.
- Guéguen C. and Cuss C. W. (2011) Characterization of aquatic dissolved organic matter by asymmetrical flow field-flow

- fractionation coupled to UV–Visible diode array and excitation emission matrix fluorescence. *J. Chromatogr. A* **1218**, 4188–4198, http://dx.doi.org/10.1016/j.chroma.2010.12.038.
- Guéguen C., Guo L. and Tanaka N. (2005) Distributions and characteristics of colored dissolved organic matter in the Western Arctic Ocean. Cont. Shelf Res. 25, 1195–1207. http:// dx.doi.org/10.1016/j.csr.2005.01.005.
- Guo L. and Santschi P. H. (1996) A critical evaluation of the crossflow ultrafiltration technique for sampling colloidal organic carbon in seawater. *Mar. Chem.* 55, 113–127. http://dx.doi.org/ 10.1016/S0304-4203(96)00051-5.
- Guo L. and Santschi P. H. (1997a) Composition and cycling of colloids in marine environments. Rev. Geophys. 35, 17–40.
- Guo L. and Santschi P. H. (1997b) Isotopic and elemental characterization of colloidal organic matter from the Chesapeake Bay and Galveston Bay. *Mar. Chem.* **59**, 1–15.
- Guo L. and Santschi P. H. (2007) Ultrafiltration and its applications to sampling and characterisation of aquatic colloids. In *IUPAC Series on Analytical and Physical Chemistry of Environmental Systems* (eds. K. J. Wilkinson and J. R. Lead), pp. 159–221. Environmental colloids and particles. John Wiley and Sons, Ltd, Chapter 4.
- Guo L., Santschi P. H. and Warnken K. W. (1995) Dynamics of dissolved organic carbon (DOC) in oceanic environments. *Limnol. Oceanogr.* 40, 1392–1403. http://dx.doi.org/10.4319/ lo.1995.40.8.1392.
- Guo L., Santschi P. H., Cifuentes L. A., Trumbore S. E. and Southon J. (1996) Cycling of high-molecular-weight dissolved organic matter in the Middle Atlantic Bight as revealed by carbon isotopic (¹³C and ¹⁴C) signatures. *Limnol. Oceanogr.* 41, 1242–1252. http://dx.doi.org/10.4319/lo.1996.41.6.1242.
- Guo L., Santschi P. H. and Bianchi T. S. (1999) Dissolved organic matter in estuaries of the Gulf of Mexico. In *Biogeochemistry of Gulf of Mexico Estuaries*. Wiley, pp. 222–240.
- Hansell D. A. (2013) Recalcitrant dissolved organic carbon fractions. Ann. Rev. Mar. Sci. 5, 421–445. http://dx.doi.org/ 10.1146/annurev-marine-120710-100757.
- Hedges J. I. (2002) Why dissolved organic matter? In Biogeochemistry of Marine Dissolved Organic Matter (eds. D. A. Hansell and C. A. Carlson). Academic Press, San Diego, London, UK.
- Hernes P. J., Bergamaschi B. A., Eckard R. S. and Spencer R. G.
 M. (2009) Fluorescence-based proxies for lignin in freshwater dissolved organic matter. J. Geophys. Res. Biogeosci. 114, G00F03
- Honeyman B. D. and Santschi P. H. (1989) A Brownian-pumping model for oceanic trace metal scavenging: evidence from Th isotopes. J. Mar. Res. 47, 951–992.
- Huguet A., Vacher L., Relexans S., Saubusse S., Froidefond J. M. and Parlanti E. (2009) Properties of fluorescent dissolved organic matter in the Gironde Estuary. *Org. Geochem.* 40, 706–719. http://dx.doi.org/10.1016/j.orggeochem.2009.03.002.
- Keown M. P., Dardeau, Jr., E. A. and Causey E. M. (1986) Historic trends in the sediment flow regime of the Mississippi river. Water Resour. Res. 22, 1555–1564. http://dx.doi.org/ 10.1029/WR022i011p01555.
- Lead J. R. and Wilkinson K. J. (2006) Aquatic colloids and nanoparticles: current knowledge and future trends. *Environ. Chem.* 3, 159–171.
- Lin P., Chen M. and Guo L. (2012) Speciation and transformation of phosphorus and its mixing behavior in the Bay of St. Louis estuary in the northern Gulf of Mexico. *Geochim. Cosmochim. Acta* 87, 283–298. http://dx.doi.org/10.1016/j.gca.2012.03.040.
- Maie N., Scully N. M., Pisani O. and Jaffé R. (2007) Composition of a protein-like fluorophore of dissolved organic matter in coastal wetland and estuarine ecosystems. *Water Res.* **41**, 563–570. http://dx.doi.org/10.1016/j.watres.2006.11.006.

- Mantoura R. F. C. and Woodward E. M. S. (1983) Conservative behaviour of riverine dissolved organic carbon in the Severn Estuary: chemical and geochemical implications. *Geochim. Cosmochim. Acta* 47, 1293–1309.
- Mattsson T., Kortelainen P. and Raike A. (2005) Export of DOM from Boreal catchments: impacts of land use cover and climate. *Biogeochemistry* **76**, 373–394.
- Meade R. H., Yuzyk T. R. and Day T. J. (1990) Movement and storage of sediment in rivers of the United States and Canada. In *Surface Water Hydrology* (eds. M. G. Wolman and H. C. Riggs). Geological Society of America, Boulder, Colorado.
- Morey S. L., Schroeder W. W., O'Brien J. J. and Zavala-Hidalgo J. (2003) The annual cycle of riverine influence in the eastern Gulf of Mexico basin. *Geophys. Res. Lett.* 30, 1867.
- Philippe A. and Schaumann G. E. (2014) Interactions of dissolved organic matter with natural and engineered inorganic colloids: a review. *Environ. Sci. Technol.* 48, 8946–8962.
- Shiller A. M., Shim M.-J., Guo L., Bianchi T. S., Smith R. W. and Duan S. (2012) Hurricane Katrina impact on water quality in the East Pearl River, Mississippi. *J. Hydrol.* **414–415**, 388–392.
- Sholkovitz E. R. (1976) Flocculation of dissolved organic and inorganic matter during the mixing of river water and seawater. *Geochim. Cosmochim. Acta* 40, 831–845.
- Stedmon C. A. and Bro R. (2008) Characterizing dissolved organic matter fluorescence with parallel factor analysis: a tutorial. *Limnol. Oceanogr. Methods* 6, 572–579. http://dx.doi.org/ 10.4319/lom.2008.6.572.
- Stolpe B., Guo L., Shiller A. M. and Aiken G. R. (2013) Abundance, size distributions and trace-element binding of organic and iron-rich nanocolloids in Alaskan rivers, as revealed by field-flow fractionation and ICP-MS. Geochim. Cosmochim. Acta 105, 221–239.
- Stolpe B., Guo L., Shiller A. M. and Hassellöv M. (2010) Size and composition of colloidal organic matter and trace elements in the Mississippi River, Pearl River and the northern Gulf of Mexico, as characterized by flow field-flow fractionation. *Mar. Chem.* 118, 119–128.
- Stolpe B., Zhou Z., Guo L. and Shiller A. M. (2014) Colloidal size distribution of humic- and protein-like fluorescent organic matter in the northern Gulf of Mexico. *Mar. Chem.* 164, 25–37. http://dx.doi.org/10.1016/j.marchem.2014.05.007.
- Wang X., Cai Y. and Guo L. (2010) Preferential removal of dissolved carbohydrates during estuarine mixing in the Bay of Saint Louis in the northern Gulf of Mexico. *Mar. Chem.* 119, 130–138.
- Wang X., Cai Y. and Guo L. (2013) Variations in abundance and size distribution of carbohydrates in the lower Mississippi River, Pearl River and Bay of St Louis. *Estuar. Coast. Shelf Sci.* 126, 61–69.
- Weishaar J. L., Aiken G. R., Bergamaschi B. A., Fram M. S., Fujii R. and Mopper K. (2003) Evaluation of specific ultraviolet absorbance as an indicator of the chemical composition and reactivity of dissolved organic carbon. *Environ. Sci. Technol.* 37, 4702–4708. http://dx.doi.org/10.1021/es030360x.
- Wiener J. G., Fremling C. R., Korschgen C. E., Kenow K. P., Kirsch E. M., Rogers S. J., Yin Y. and Sauer J. S. (1996) Mississippi River, Status and Trends of Nation's Biological Resources. National Weather Resources Center, U.S. Geological Survey, Washington, D.C.
- Williams C. J., Yamashita Y., Wilson H. F., Jaffé R. and Xenopoulos M. A. (2010) Unraveling the role of land use and microbial activity in shaping dissolved organic matter characteristics in stream ecosystems. *Limnol. Oceanogr.* 55, 1159– 1171
- Williams P. S., Xu Y., Reschiglian P. and Giddings J. C. (1997) Colloid characterization by sedimentation field-flow fractiona-

- tion-correction for particle-wall interaction. *Anal. Chem.* **69**, 349–360.
- Yamashita Y. and Tanoue E. (2003) Chemical characterization of protein-like fluorophores in DOM in relation to aromatic amino acids. *Mar. Chem.* 82, 255–271.
- Zanardi-Lamardo E., Clark C. D., Moore C. A. and Zika R. G. (2002) Comparison of the molecular mass and optical properties of colored dissolved organic material in two rivers and coastal waters by Flow Field-Flow Fractionation. *Environ. Sci. Technol.* **36**, 2806–2814.
- Zhou Z. and Guo L. (2015) A critical evaluation of an asymmetrical flow field-flow fractionation system for colloidal size
- characterization of natural dissolved organic matter. *J. Chromatogr. A* **1399**, 53–64. http://dx.doi.org/10.1016/j.chroma.2015.04.035.
- Zhou Z., Guo L., Shiller A. M., Lohrenz S. E., Asper V. L. and Osburn C. L. (2013) Characterization of oil components from the Deepwater Horizon oil spill in the Gulf of Mexico using fluorescence EEM techniques. *Mar. Chem.* 148, 10–21. http://dx.doi.org/10.1016/j.marchem.2012.10.003.

Associate editor: Thomas S. Bianchi